Photosensitivity of Functional Polystyrene and Poly(methyl methacrylate) Synthesized by Controlled Radical Polymerization

Suk Hang Chan,[†] Lillian Sze Man Lam,[†] Chui Wan Tse,[†] Ka Yan Kitty Man,[†] Wing Tak Wong,[†] Aleksandra B. Djurišić,[‡,§] and Wai Kin Chan*[,†]

Department of Chemistry, The University of Hong Kong, Pokfulam Road, Hong Kong, China; Department of Electrical and Electronic Engineering, The University of Hong Kong, Pokfulam Road, Hong Kong, China; Department of Physics, The University of Hong Kong, Pokfulam Road, Hong Kong, China

Received March 6, 2003; Revised Manuscript Received May 9, 2003

ABSTRACT: We report the synthesis and photosensitizing properties of various polystyrene and poly(methyl methacrylate) that contain metal complex cores. The polymers were synthesized by atom transfer radical polymerization (ATRP) using metalloinitiators based on rhenium and ruthenium diimine complexes. The detailed structures of the initiators were determined by X-ray crystallography. In ATRP, the catalyst systems were composed of copper(I) bromide and 1,1,4,7,7-pentamethyldiethylenetriamine. The rates of polymerization depended on several factors such as the amounts of initiator, copper bromide, and ligand with respect to the monomer concentration. From the kinetic plots, the polymerizations showed first-order kinetics with respect to the monomer concentration, and the typical rate of polymerization is on the order of 10^{-5} s^{-1}. The photoconducting properties of the polymers were studied using argon-ion laser (488 nm) as the light source. The metal complex cores may serve as efficient photosensitizers in the visible region, and the photoconductivities of the polymers are on the order of 10^{-10} $\Omega^{-1}cm^{-1}$. The experimental quantum yields were fitted into Onsager's equation, from which the primary yield and thermalization distance were calculated to be 0.02 and 1.3 to 1.8 nm, respectively.

Introduction

The syntheses of polymers with controlled molecular weight and architecture are of great importance to materials research.[1] Of the different controlled polymerization methods, atom transfer radical polymerization (ATRP) has attracted a great deal of interest in the past few years.[2,3] ATRP enjoys the advantages that it can tolerate polar or electrophilic functional groups. It can polymerize polar monomers in bulk or in other polar solvents.[4,5] As a result, functional homopolymers or multiblock copolymers with controlled molecular weight and morphological properties can be easily synthesized. This offers a great advantage to polymer chemists in designing novel polymeric materials with specific functions that rely heavily on the uniformity of molecular sizes.

Our research effort has long been focused on the design and synthesis of various metal-containing polymers with interesting optical or electronic properties.[6] The metal complexes incorporated in the polymer main chain or side chain can function as photosensitizers, light emitters, and charge transport species. Several diimine complexes based on d^6 transition metals exhibit very strong photosensitivities; their photocharge generation and charge transport properties were studied in detail.[7] Some of these polymers were also fabricated into photovoltaic devices.[8] However, the polymers were mainly synthesized by random step-growth copolymerization with little control over the molecular weight and extent of reaction. Recently, we showed that a metal-containing diblock copolymer formed nanosized micelles in selected solvent systems.[9] The metal complex was incorporated into the polymer after synthesizing a copolymer by anionic polymerization. However, the choice of monomer was limited, and the degree of functionalization is not easy to control. Therefore, our goal is to synthesize functional homo- or copolymers by controlled polymerization. There have been several examples of using multifunctional initiators in ATRP.[10] The syntheses of star-shaped polymers by ATRP using tris(2,2′-bipyridyl) ruthenium(II) complexes as the initiators have been reported.[11−13] Polymers synthesized by metalloinitiators using controlled polymerizations can also serve as the building blocks for supramolecular chemistry and nanotechnology.[14]

In this paper, we report the synthesis of a series of polystyrene (PS) or poly(methyl methacrylate) (PMMA) derivatives using various types of metalloinitiators based on rhenium or ruthenium diimine complexes. 1,4-Diaza-1,3-butadiene (DAB) was chosen as the ligand because complexes with this ligand can act as efficient photosensitizers.[15,16] They possess a long-lived excited state with metal-to-ligand charge-transfer character.[17] As a result, long-lived excitons are generated upon photoexcitation, which may lead to a more efficient charge generation and separation processes. The metal complex cores in these polymers are able to act as photosensitizing centers, which are encapsulated by the PS or PMMA shells. The density and hence the distance separating these photosensitizers can be fine-tuned by controlling the molecular weight of the polymers. The photoconductivities of these polymers were studied in detail, and the experimental results were fitted to a theoretical model in order to understand the mechanisms of the photocharge generation process.

* Corresponding author. E-mail: waichan@hku.hk.
[†] Department of Chemistry, The University of Hong Kong.
[‡] Department of Electrical and Electronic Engineering, The University of Hong Kong.
[§] Department of Physics, The University of Hong Kong.

10.1021/ma030161y CCC: $25.00
Published on Web 06/26/2003

Experimental Section

Materials. 2-Bromoisobutyryl bromide (97%), 4-aminophenol (98%), and 1,1,4,7,7-pentamethyldiethylenetriamine (PMDETA, 98%) were purchased from Lancaster Synthesis Ltd. Rhenium(I) pentacarbonyl chloride (98%), silver trifluoromethanesulfonate (98%), potassium hexafluorophosphate (99.5%), and copper(I) bromide (98%) were purchased from Strem Chemical Co. Glyoxal (30% aqueous solution) and anisole (99%) were purchased from Acros Chemical Co. Triethylamine (Lancaster, 99%) was distilled over calcium hydride. Xylene was distilled and stored over molecular sieves before used. Bis(2,2′-bipyridyl) ruthenium(II) dichloride dihydrate[18] was prepared according to a literature procedure. Styrene (Sty, Aldrich, 99%) and methyl methacrylate (MMA, Lancaster, 99%) were distilled under reduced pressure and stored over molecular sieves. Unless otherwise specified, all other chemicals were used as received.

Instrumentation. ^{1}H and ^{13}C NMR spectra were collected on Bruker AM-500 (500 MHz) or Bruker DPX-300 (300 MHz) NMR spectrometers. UV−vis spectra were collected on a Hewlett-Packard HP8452 photodiode array spectrophotometer. FTIR spectra (KBr pellets) were collected on a Bio-Rad FTS-7 FTIR spectrometer. Mass spectrometry was performed on a high-resolution Finnigan MAT-95 mass spectrometer. Melting point measurements and thermal analyses were performed on a Perkin-Elmer DSC7 and TGA7 thermal analyzers under a nitrogen atomsphere with the heating rate of 10 and 15 °C/min, respectively. The DSC was calibrated using indium metal as the reference. Molecular weights were determined using a GPC system equipped with an ISCO 2350 pump, an ISCO V4 absorbance detector, and a Viscotek 250 viscosity/refractive index dual detector. Two Ultrastyragel columns with bead sizes of 10 μm and pore sizes of 1000 Å (for MW = 1000−20000) and 10000 Å (for MW = 10000−200000) were used. THF was used as the eluent with a flow rate of 1.0 mL/min at 35 °C. It was calibrated against polystyrene narrow standards. Gas chromatography was performed on a Hewlett-Packard HP5890 gas chromatograph equipped with an Ultra-1 column (cross-linked methyl silicone gum, 25 m × 0.32 mm × 0.52 μm film thickness) and a flame ionization detector. Helium was used as the carrier gas. Both injector and detector temperatures were set at 160 °C. After injecting the sample, the system was kept at 60 °C for 15 min. Then it was increased at a rate of 20 °C/min to 230 °C at which it was kept for 30 min.

Photoconductivity Measurements. The polymer films for photoconductivity measurements were prepared by spin coating the polymer solution (with or without dopants) in 1,1,2,2-tetrachloroethane onto indium−tin−oxide-coated glass slides (2.5 × 2.5 cm). The thickness of the polymer films was measured by a Dektak 3ST surface profiler and typical thickness of the films was 0.5 μm. An aluminum electrode (0.1 μm) was then coated on the polymer film surface by thermal evaporation under high vacuum (6×10^{-6} mbar). Upon irradiation with an argon-ion laser (488 nm, 5 mW), the photocurrent response was measured from the voltage drop across a resistor with a lock-in amplifier (Stanford Research SR 510) in the presence of an applied electric field. The detailed experimental setup has been reported elsewhere.[19]

1,4-Bis(4-hydroxyphenyl)-1,4-diaza-1,3-butadiene, 1. A mixture of 4-aminophenol (2.43 g, 22 mmol) and glyoxal (30% aqueous solution, 1.62 g, 27 mmol) was refluxed in ethanol (10 mL) under a nitrogen atmosphere for 24 h. The yellow product was filtered and washed with ethanol until the filtrate was clear. The product was used for the next reaction without further purifications. Yield: 1.52 g (23%). Mp: 208.5 °C (DSC). ^{1}H NMR (DMSO-d_6), δ: 9.78 (s, 2H, OH), 8.40 (s, 2H, N=C−H), 7.32 (d, J = 8.7 Hz, 4 H, Ar−H), 6.82 (d, J = 8.7 Hz, 4 H, Ar−H). ^{13}C NMR (DMSO-d_6), δ: 157.7, 156.3, 141.1, 123.2, 115.8. FTIR (KBr), cm^{-1}: ν = 1608 (C=N stretching), 833 (C−H out-of-plane bending, 1,4-disubstituted benzene). UV−vis (DMF), λ_{max}/nm (ϵ/dm^3 mol^{-1}cm^{-1}): 382 (16550). MS, *m*/*e*: 240 (M^+).

Chlorotricarbonyl[1,4-bis(4-hydroxyphenyl)-1,4-diaza-1,3-butadiene]rhenium(I), 2. A mixture of rhenium(I) pentacarbonyl chloride (0.50 g, 1.3 mmol) and **1** (0.34 g, 1.3 mmol) were refluxed in toluene (5 mL) under a nitrogen atmosphere for 24 h. The red precipitate was filtered and washed with toluene and ether. It can be purified by dissolving the crude product in chloroform and reprecipitated in ether. Yield: 0.73 g (96%). Mp: 311 °C dec (TGA). ^{1}H NMR (DMSO-d_6), δ: 10.23 (s, 2H, OH), 8.83 (s, 2H, N=C−H), 7.46 (d, J = 8.8 Hz, 4 H, Ar−H), 6.94 (d, J = 8.8 Hz, 4 H, Ar−H). ^{13}C NMR (DMSO-d_6), δ: 196.7, 185.5, 164.6, 159.2, 142.2, 124.2, 115.8. FTIR (KBr), cm^{-1}: ν = 2021, 1929, 1900 (metal carbonyl CO stretching), 1610 (C=N stretching), 835 (C−H out-of-plane bending, 1,4-disubstituted benzene). UV−vis (DMF), λ_{max}/nm (ϵ/dm^3 mol^{-1}cm^{-1}): 440 (12750), 681 (4120). FABMS, *m*/*e*: 546 (M^+).

Chlorotricarbonyl[1,4-bis(2-bromoisobutyryloxyphenyl)-1,4-diaza-1,3-butadiene]rhenium(I), 3. In a nitrogen atmosphere, complex **2** (0.50 g, 0.92 mmol), triethylamine (0.46 g, 4.6 mmol), and 2-bromoisobutyryl bromide (0.28 mL, 2.3 mmol) were dissolved in distilled THF (5 mL) and the mixture was stirred for 3 h at 25 °C. The solvent was removed under reduced pressure and the residue was extracted with CH_2Cl_2. The organic layer was washed with water and then dried over anhydrous magnesium sulfate. The solvent was removed, and the red product was purified by recrystallization with ethanol. Yield: 0.53 g (68.6%). Mp: 182 °C (DSC). ^{1}H NMR ($CDCl_3$), δ: 8.72 (s, 2H, N=C−H), 7.57 (d, J = 8.9 Hz, 4 H, Ar−H), 7.33 (d, J = 8.9 Hz, 4 H, Ar−H), 2.10 (s, 12 H, CH_3). ^{13}C NMR ($CDCl_3$), δ: 195.1, 182.5, 169.9, 163.6, 152.0, 148.7, 123.5, 122.6, 54.9, 30.5. FTIR (KBr), cm^{-1}: ν = 2032, 1936, 1911 (metal carbonyl CO stretching), 1749 (C=O stretching), 1610 (C=N stretching). UV−vis ($CHCl_3$), λ_{max}/nm (ϵ/dm^3 mol^{-1} cm^{-1}): 385 (10530), 521 (4520). FABMS, *m*/*e*: 844 (M^+). Anal. Calcd for $C_{25}H_{22}O_7N_2Br_2ClRe$: C, 35.58; H, 2.63; N, 3.32. Found: C, 35.01; H, 2.43; N, 3.11.

[1,4-Bis(4-hydroxyphenyl)-1,4-diaza-1,3-butadiene]bis-(2,2′-bipyridyl)ruthenium(II) Hexafluorophosphate, 4. Bis(2,2′-bipyridyl)ruthenium(II) dichloride dihydrate (0.50 g, 0.9 mmol) was added to silver trifluoromethanesulfonate (0.50 g, 1.9 mmol) in acetone (10 mL) under a nitrogen atmosphere. The mixture was stirred at 25 °C for 3 h and the silver chloride formed was filtered off. The filtrate was evaporated to dryness yielding the $[Ru(bpy)_2(acetone)_2](SO_3CF_3)_2$. Compound **1** (0.21 g, 0.9 mmol) and ethanol (10 mL) were then added and the mixture was refluxed for 24 h. The solution was concentrated and then added to an aqueous potassium hexafluorophosphate solution. The red precipitate was filtered and the crude product was purified by recrystallization with ethanol. Yield: 0.59 g (59%). Mp: 278 °C (DSC). ^{1}H NMR (DMSO-d_6), δ: 9.86 (s, 2 H, OH), 8.95 (s, 2 H, N=C−H), 8.63 (d, J = 8.6 Hz, 2 H, bpy-H), 8.50 (d, J = 8.3 Hz, 2 H, bpy-H), 8.28 (t, J = 7.5 Hz, 4 H, bpy-H), 8.00 (t, J = 7.8 Hz, 2 H, bpy-H), 7.79 (t, J = 6.9 Hz, 2 H, bpy-H), 7.64 (d, J = 5.5 Hz, 4 H, bpy-H), 7.38 (t, J = 7.0 Hz, 2 H, bpy-H), 6.45 (d, J = 8.9 Hz, 4 H, Ar−H), 6.37 (d, J = 8.9 Hz, 4 H, Ar−H). ^{13}C NMR (DMSO-d_6), δ: 165.1, 158.2, 156.2, 155.7, 152.8, 151.3, 141.6, 138.9, 138.5, 128.7, 127.7, 124.1, 123.9, 123.2, 115.4. FTIR (KBr), cm^{-1}: ν = 1605 (C=N stretching), 844 (P−F stretching). UV−vis (MEK), λ_{max}/nm (ϵ/dm^3 mol^{-1}cm^{-1}): 414 (9430), 450(7540). FABMS, *m*/*e*: 798 (M-$2PF_6$)$^+$.

[1,4-Bis(2-bromobutyryloxyphenyl)-1,4-diaza-1,3-butadiene]bis(2,2′-bipyridyl)ruthenium(II) Hexafluorophosphate, 5. It was prepared according to a procedure similar to that described in the synthesis of **3**. Yield: 90%. Mp: 204 °C (DSC). ^{1}H NMR (DMSO-d_6), δ: 9.21 (s, 2 H, N=C−H), 8.64 (d, J = 8.8 Hz, 2 H, bpy-H), 8.49 (d, J = 7.6 Hz, 2 H, bpy-H), 8.38 (d, J = 5.6 Hz, 2 H, bpy-H), 8.32 (t, J = 8.0 Hz, 4 H, bpy-H), 7.99 (t, J = 7.4 Hz, 2 H, bpy-H), 7.84 (t, J = 7.1 Hz, 2 H, bpy-H), 7.63 (d, J = 5.1 Hz, 4 H, bpy-H), 7.38 (t, J = 6.4 Hz, 2 H, bpy-H), 6.88 (d, J = 8.5 Hz, 4 H, Ar−H), 6.70 (d, J = 8.5 Hz, 4 H), 2.08 (s, 12 H, CH_3). ^{13}C NMR (DMSO-d_6), δ: 169.2, 167.8, 155.7, 155.1, 152.9, 150.9, 149.9, 146.8, 139.0, 138.4, 128.6, 127.6, 123.9, 123.8, 122.8, 121.6, 29.8. FTIR (KBr), cm^{-1}: ν = 1755 (C=O stretching), 843 (P−F stretching).

Scheme 1. Synthesis of Initiators 3 and 5

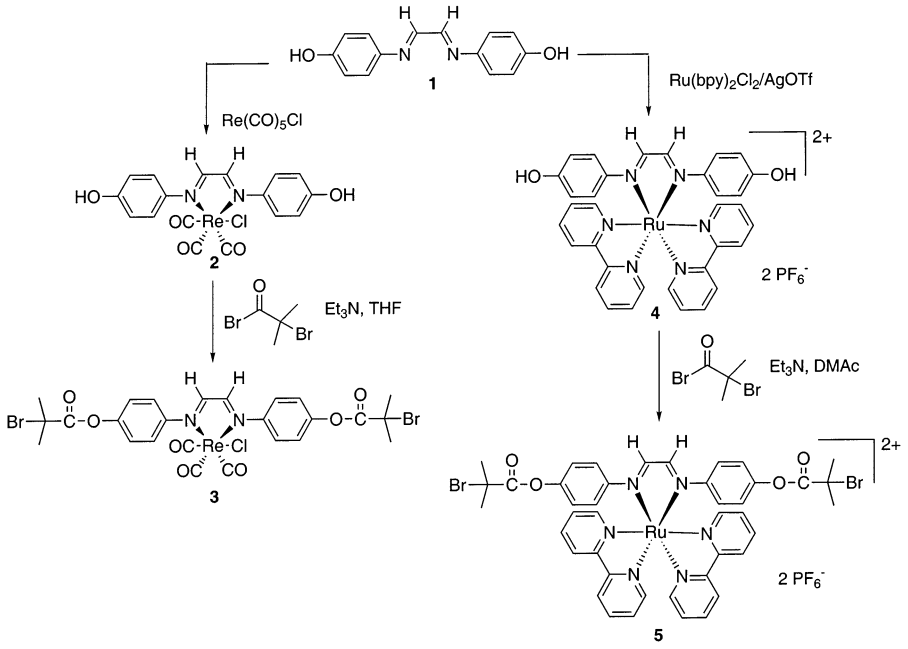

UV−vis (MEK), λ_{max}/nm (ϵ/dm^3 mol^{-1}cm^{-1}): 327 (13430), 493 (8360). FABMS, *m*/*e*: 952 (M − 2PF_6)$^+$. Anal. Calcd for $C_{42}H_{38}O_4N_6Br_2P_2F_{12}Ru$: C, 40.63; H, 3.08; N, 6.77. Found: C, 40.08; H, 3.32; N, 6.51.

Synthesis of Polymers from Metalloinitiators. The synthesis of Re−MMA is described as general procedure for the polymerization kinetic studies. Copper(I) bromide (28 mg, 0.19 mmol) and PMDETA (34 mg, 0.19 mmol) were added to a Schlenk flask filled with nitrogen. MMA (3.6 mL, 34 mmol) and anisole (5% v/v relative to monomer as an internal GC standard) were added to the flask via a gastight syringe. The solution polymerization was performed using the same procedure except that distilled xylene was used as the solvent (1:1 v/v vs MMA). The reaction mixture was degassed by three freeze−pump−thaw cycles and the mixture was stirred at room temperature for 12 h. Complex **3** was added to the mixture and the solution was degassed again by three freeze−pump−thaw cycles. The flask was sealed and placed into an oil bath at 40 °C for 1.5 h. It was precipitated into methanol at the end of the reaction. The crude product was dissolved in methylene chloride, and the solution was passed through an alumina column to remove the copper catalyst. It was reprecipitated into methanol and the product was collected by filtration. Yield: 2.1 g (62% conversion). By using GPC, the number-average molecular and polydispersity were measured to be 26 000 and 1.41, respectively. For the polymerization kinetic study, the polymerization was stopped by immersing the flask in an ice−water bath at different time interval. A small aliquot was taken from the reaction mixture and it was dissolved in methylene chloride. The solution was filtered with a 0.2 μm membrane filter and the extent of conversion was analyzed by gas chromatography. After removal of the solvent, THF was added to dissolve the polymer and its molecular weight was measured by GPC.

X-ray Crystallography. Single crystals of **3** and **5** were prepared by layer diffusion between hexane and chloroform solution (for **3**) or between benzene and DMF solution (for **5**). The crystals were mounted in capillaries or glass fiber and the crystal structures were determined with a Bruker AXS SMART-CCD diffractometer with graphite monochromated Mo Kα radiation (λ = 0.710 73 Å) and a 12 kW rotating anode generator. Data were collected using the ω−2θ scan technique to a maximum 2θ value of 50.0 °. The structures were solved by direct methods[20] and expanded using Fourier techniques.[21] The crystal data of initiators **3** and **5** are available as Supporting Information in CIF format.

Results and Discussion

Synthesis and Characterizations of Initiators and Polymers. Metalloinitiators **3** and **5** were synthesized by the reaction between hydroxy-substituted metal diimine complexes **2** (in THF) and **4** (in DMAc), respectively with 2-bromoisobutyryl bromide (Scheme 1). The structures of the initiators were confirmed by various spectroscopic techniques and X-ray crystallography. In the NMR spectra, complexes **3** and **5** show a sharp singlet at 8.72 and 9.21, respectively, which corresponds to the imine proton (N=C−H) of the ligand. In the FTIR spectra, initiator **3** shows three very strong CO stretching bands at 2032, 1936, and 1911 cm^{-1}. This confirms the presence of the *facial* rhenium carbonyl ligands.[22] These characteristic absorption bands can be used as very good fingerprints for confirming the presence of metal complex initiator in the polymers (vide infra). The stretching band at ca. 1750 cm^{-1} in both initiators also confirms the presence of ester carbonyl group. In their UV−vis absorption spectra, they show intense absorption bands at 521 and 493 nm, respectively. These are attributed to the characteristic metal-to-ligand charge transfer transition of the metal complex. The geometries of the initiators were unambiguously confirmed by X-ray crystallography. The structures of **3** and **5** with atomic numbering are depicted in Figures 1 and 2, and selected bond distances and angles are summarized in Tables 1 and 2, respectively. Complex **3** exhibits a distorted octahedral coordination, as evidenced by the significant reduction of the N−Re−N angle from 90° in the idealized polyhedron to 76.2(4)°, and the trans angles about rhenium atom ranges from 167.6(6) to 172.8(6)°. These distortions most likely result from packing forces and electronic and steric effects associated with twisting of the phenylene units, which are not coplanar to the diimine moiety. The dihedral angles between the two phenyl rings and the diimine unit are 82.1 and 40.7°. The carbonyl groups assume a *facial* geometry about the metal center with the Re−C bond distances range from 1.79(2) to 1.87(2) Å, which are shorter than those of similar rhenium carbonyl complexes. On the other hand, the C−O distances in the carbonyl ligands range

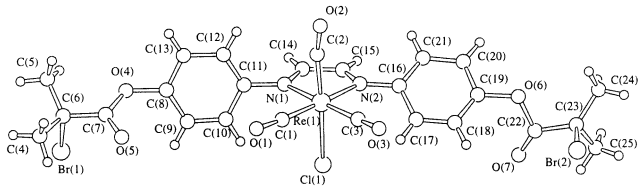

Figure 1. Perspective drawing of initiator **3** with the atomic numbering scheme.

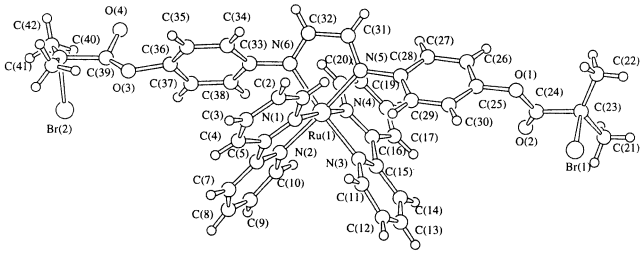

Figure 2. Perspective drawing of initiator **5** with the atomic numbering scheme.

Table 1. Selected Geometric Data for Initiator 3

	Bond Length (Å)		
Re(1)−Cl(1)	2.518(4)	Re(1)−N(1)	2.14(1)
Re(1)−N(2)	2.14(1)	Re(1)−C(1)	1.79(2)
Re(1)−C(2)	1.81(3)	Re(1)−C(3)	1.87(2)
Br(1)−C(6)	2.01(2)	Br(2)−C(23)	1.966(9)
Br(2)−C(26)	0.560(3)	Br(3)−C(23)	2.015(9)
BR(3)−C(25)	0.77(1)	O(1)−C(1)	1.23(2)
O(2)−C(2)	1.23(2)	O(3)−C(3)	1.20(2)
N(1)−C(14)	1.31(2)	C(14)−C(15)	1.41(2)
	Bond Angle (deg)		
Cl(1)−Re(1)−N(1)	83.7(4)	Cl(1)−Re(1)−N(2)	82.8(4)
Cl(1)−Re(1)−C(1)	90.9(6)	Cl(1)−Re(1)−C(2)	169.7(7)
Cl(1)−Re(1)−C(3)	92.6(6)	N(1)−Re(1)−N(2)	76.2(4)
N(1)−Re(1)−C(1)	92.5(7)	N(1)−Re(1)−C(2)	86.6(8)
N(1)−Re(1)−C(3)	172.8(6)	N(2)−Re(1)−C(1)	167.6(6)
N(2)−Re(1)−C(2)	91.6(8)	N(2)−Re(1)−C(3)	97.3(6)
C(1)−Re(1)−C(2)	92.9(10)	C(1)−Re(1)−C(3)	93.7(8)
C(2)−Re(1)−C(3)	96.7(9)	Re(1)−N(1)−C(14)	113.9(10)
Re(1)−N(2)−C(15)	114.1(10)		

Table 2. Selected Geometric Data for Initiator 5

	Bond Length (Å)		
Ru(1)−N(1)	2.06(2)	Ru(1)−N(2)	2.07(1)
Ru(1)−N(3)	2.10(1)	Ru(1)−N(4)	2.08(1)
Ru(1)−N(5)	2.05(1)	Ru(1)−N(6)	2.05(2)
Br(1)−C(23)	2.01(2)	Br(2)−C(40)	2.06(3)
P(1)−F(1)	1.46(2)	P(1)−F(6)	1.48(2)
P(2)−F(7)	1.46(2)	P(2)−F(12)	1.56(2)
O(2)−C(24)	1.21(2)	O(4)−C(39)	1.26(4)
O(1)−C(24)	1.28(2)	O(3)−C(39)	1.22(3)
N(6)−C(32)	1.27(2)	C(31)−C(32)	1.40(2)
	Bond Angle (deg)		
N(1)−Ru(1)−N(2)	77.5(6)	N(1)−Ru(1)−N(3)	98.9(6)
N(1)−Ru(1)−N(4)	174.3(6)	N(1)−Ru(1)−N(5)	100.2(6)
N(1)−Ru(1)−N(6)	83.5(5)	N(2)−Ru(1)−N(3)	85.1(5)
N(2)−Ru(1)−N(4)	97.0(6)	N(2)−Ru(1)−N(5)	176.4(6)
N(2)−Ru(1)−N(6)	100.2(6)	N(3)−Ru(1)−N(4)	79.0(5)
N(3)−Ru(1)−N(5)	98.0(5)	N(3)−Ru(1)−N(6)	174.6(6)
N(4)−Ru(1)−N(5)	85.3(5)	N(4)−Ru(1)−N(6)	99.1(6)
N(5)−Ru(1)−N(6)	76.7(6)	F(1)−P(1)−F(2)	91(1)
F(7)−P(2)−F(8)	95(1)	F(1)−P(1)−F(6)	177(1)
F(11)−P(2)−F(12)	92(1)		

from 1.20(2) to 1.23(2) Å and are shorter than those reported in the literature.[23] This indicates an increasing mixing between the dπ orbitals of the rhenium atom and the π* orbitals of the carbonyl ligands. The Re−N distances are identical with a value of 2.14(1) Å. This is shorter than the Re−N distances found in other

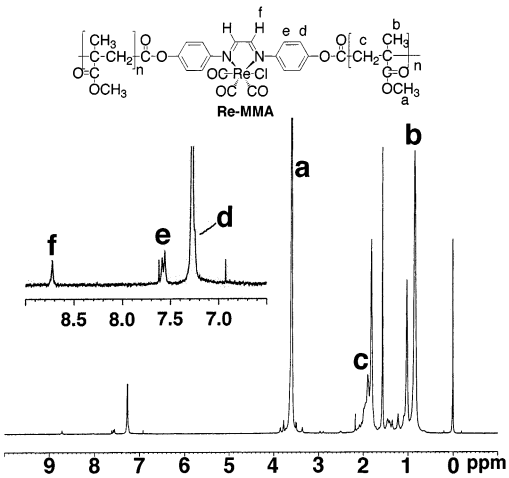

Figure 3. ^{1}H NMR spectrum of Re−MMA in $CDCl_3$. One of the peaks due to the phenylene protons on the initiator (~7.2 ppm) is partially masked by the solvent peak.

rhenium tricarbonyl complexes based on aromatic diimine ligands.[24] Again, it suggests lower-lying π* orbitals in the diimine ligands which results in stronger back-bonding by the rhenium atom. Another interesting structural feature is that there is disorder in the crystal packing. Because of the similar steric demand of the bromine atom and the methyl group, there are two types of crystal packing and the positions of the Br(2) and C(25) are not fixed.

Complex **5** also has a slightly distorted octahedral coordination. The N−Ru−N biting angles of the three diimine ligands range from 76.7(6) to 79.0(5)°, and the trans angles range from 174.3(6) to 176.4(6)°, indicating that the geometry is less distorted than that of complex **3**. The dihedral angles between the diimine unit and the phenyl rings are quite similar (53.7 and 57.2°). There was only one type of crystal packing for this complex.

The presence of metal complex moieties in the polymers was characterized by spectroscopic methods. The ^{1}H NMR spectrum of Re−MMA is shown in Figure 3. The spectral features are very similar to PMMA, except that there are three sets of small peaks due to the initiators in the aromatic region. The singlet at 8.7 ppm is due to the imine protons on the rhenium complex, while the other two peaks are ascribed to the phenylene protons. Although the peak at ca. 7.2 ppm is masked by the solvent peak, there is an obvious shoulder. From the FTIR spectra, both Re−Sty and Re−MMA show three metal carbonyl stretching peaks at 2020, 1930, and 1900 cm^{-1}. For Ru−Sty and Ru−MMA, the P−F stretching band due to the counteranion is at 844 cm^{-1}. The UV−vis absorption spectra of these polymers are almost the same as those for pure polystyrene or PMMA, except that there is an small absorption band at 500 nm due to the presence of the metal complex on the polymer chain. The GPC traces of the eluted polymer observed with the inline UV−vis photodiode array detector are very similar to those of the initiators. All these results support the existence of metal complex cores in the polymers and there was no change in the metal complexes during the polymerization.

Syntheses of Re—Sty and Ru—Sty. The experimental details of the polymerizations and the results are summarized in Table 3. The syntheses of Re−Sty and Ru−Sty were carried out in bulk using complexes **3** and **5**, respectively, as the initiators (Scheme 2) at 95

Table 3. Detailed Experimental Conditions and Results for the Polymerizations of Sty and MMA Initiated by 3 and 5[e]

entry	initiator	monomer	[M]/[CuBr]/[PMDETA]/[I]	time (h)	convn (%)[a]	$k_{app} \times 10^5$ (s^{-1})	M_n(calcd) $\times 10^{-3}$	M_n(GPC)[b] $\times 10^{-3}$	M_n(NMR) $\times 10^{-3}$	M_w/M_n
1	**3**	Sty	176/1/1/0.1	25.7	49	0.66	87.2	228	183	1.52
2	**3**	Sty	176/1/1/0.25	10.3	34	0.95	26.1	76.8	59.2	1.46
3	**3**	Sty	176/1/1/0.5	10.4	33	1.04	12.8	41.2	30.0	1.23
4	**3**	Sty	176/1/2/0.5	10.1	38	1.24	14.7	36.4	26.0	1.21
5	**3**	Sty	176/1/1/1	10.3	36	1.05	7.7	22.9	15.0	1.26
6	**3**	MMA	176/1/1/0.5	1.5	62	17	22.6	26.0	25.3	1.41
7	**3**	MMA in xylene	176/1/1/0.5	5.8	64	5.10	23.4	34.6	50.0	1.50
8	**5**	Sty	176/1/1/0.5	42.6	80	0.45	30.5	42.7	*c*	1.12
9	**5**	Sty	176/1/2/0.5	8.7	69	2.7	26.5	31.3	*c*	1.12
10	**5**	MMA	176/1/1/0.5	1.1	67	38	24.6	18.8	22.2[d]	1.38

[a] Monomer conversions were measured by GC using anisole as the internal standard. [b] Molecular weights and polydispersities were determined by GPC relative to polystyrene using THF as the eluent. [c] Molecular weights of polystyrene synthesized from complex **5** could not be estimated from NMR because the signals of the bipyridyl protons overlap with those of polystyrene. [d] Molecular weight was estimated by comparing the integration of the bipyridyl protons to those of the $-OCH_3$ units in MMA. [e] All of the polymerizations were carried in bulk except entry 7.

Scheme 2. Polymerization of Sty and MMA Using Various Metalloinitiators

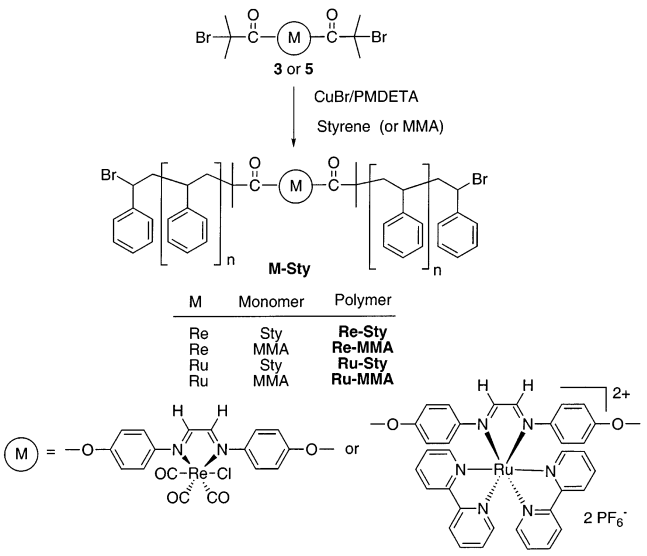

°C. A mixture of CuBr/PMDETA was used as the catalyst because of its high solubility and reactivity.[25] In addition, if 2,2′-bipyridine or its derivatives are used, they undergo ligand exchange with the diimine ligands of the initiators.[26] The catalyst-to-initiator ratios were [Sty]/[CuBr]/[PMDETA]/[I] = 176/1/1/[I], where the concentrations of the initiator were varied from 0.1 to 1 equiv with respect to [CuBr] (entries 1 to 5). The semilogarithmic plots of monomer conversion vs time suggest that the kinetics are first order with respect to the monomer concentration and that radical concentrations are constant during the reactions (Figure 4). The polymerization with [I]/[Cu] = 0.1 has the slowest reaction rate as expected ($k_{app} = 6.6 \times 10^{-6}$ s^{-1}). Increasing the [I]/[Cu] ratio from 0.25 to 1 slightly increases the rate of polymerization ($k_{app} \sim 1 \times 10^{-5}$ s^{-1}; entries 3−5). The reaction rates are comparable to the kinetic data for the ATRP of styrene using alkyl bromide as the initiator.[3,4]

Figure 5 shows the molecular weight and polydispersity of Re−Sty as functions of monomer conversion under various initiator concentrations. The molecular weight increases linearly with conversion up to approximately 33−50% for polymerizations with [I]/[Cu] = 0.25, 0.5, and 1. In general, the polydispersities of the polymers obtained from these bifunctional initiators are slightly higher than those monofunctional initiators reported in the literature.[27] The molecular weights of

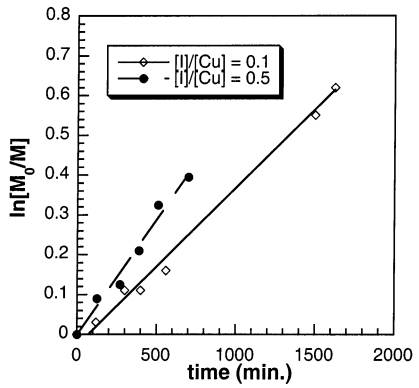

Figure 4. Plot of ln [M_0/M] vs time for the bulk polymerization of Sty at 95 °C initiated by complex **3** with different initiator concentrations. $[Sty]_0 = 8.7$ M (bulk); $[CuBr]_0 = [PMDETA]_0 = 0.05$ M.

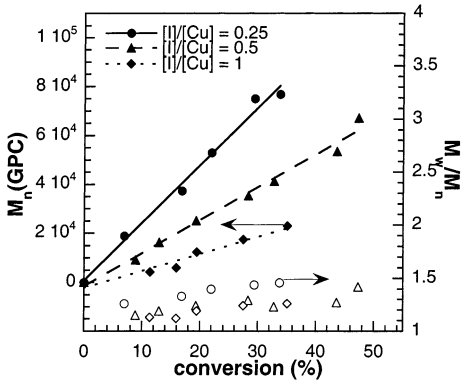

Figure 5. Plot of M_n and M_w/M_n vs conversion for the bulk polymerization of Sty at 95 °C initiated by complex **3** with different initiator concentrations. The filled data points are for M_n values and the open data points are for polydispersities. See Figure 4 for conditions.

the polymers measured by GPC are consistently higher than their theoretical values. One possible reason is that linear PS standards for GPC calibration do not correlate well with the polymers with metal complex cores. In addition, the low reactivity of the metalloinitiators may decrease the number of effective initiators in the system. The molecular weight of the polymers was also estimated by other methods. From the ^1H NMR spectra, the integrals of the protons of the initiator and the polystyrene may provide the number of styrene units per unitiator on the polymer chain.

In previous papers on ATRP, the ligand:copper catalyst ratio was usually kept at 1 to 2 equiv, depending

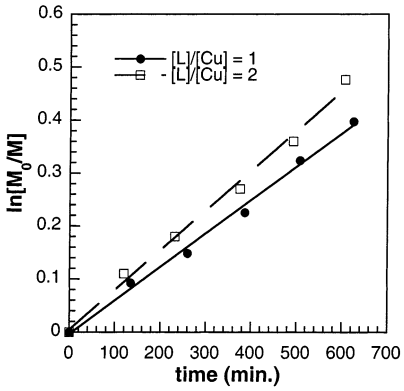

Figure 6. Plot of ln [M_0/M] vs time for the bulk polymerization of Sty at 95 °C initiated by complex **3** with different ligand concentrations. $[Sty]_0 = 8.7$ M (bulk); $[CuBr]_0 = [\mathbf{3}]_0 = 0.05$ M.

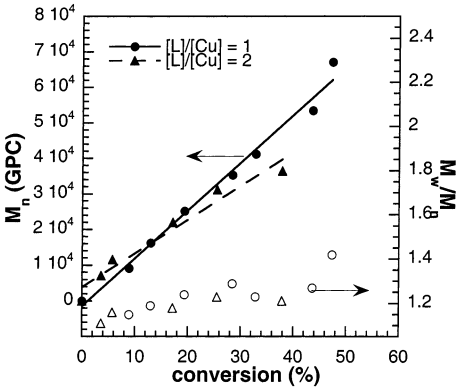

Figure 7. Plot of M_n and M_w/M_n vs conversion for the bulk polymerization of Sty at 95 °C initiated by complex **3** with different ligand concentrations. The filled data points are for M_n values and the open data points are for polydispersities. See Figure 6 for conditions.

on the nature of the ligand.[4,25] Normally, for a bidentate ligand such as TMEDA or 2,2′-bipyridine derivatives, 2 equiv of ligand was needed.[4] For multidentate ligands such as PMDETA or HMTETA, 1 to 1.5 equiv of ligand yielded satisfactory results.[25,27,28] In our work, we tested the effect of ligand concentration on the rate of polymerization. When the PMDETA concentration was increased from 1 to 2 equiv vs CuBr (entries 3−4), the rate of polymerization increased slightly. The linear kinetic plots (Figure 6) indicate that the concentration of growing radicals was constant in both cases. The M_n values also increased linearly with the conversion and low polydispersities (1.2−1.4) were maintained throughout the polymerzation (Figure 7).

Because of the ionic nature of complex **5**, its solubility is lower in the nonpolar styrene monomer, and the kinetics of polymerization are different. This may lead to inconsistencies between the theoretical and measured molecular weights. The catalyst system used in the synthesis of Ru−Sty was [Sty]/[CuBr]/[I] = 176/1/0.5, where the concentration of the ligand was varied from 1 to 2 equiv with respect to [CuBr]. Figure 8 shows the kinetics plots of ln[M_0/M] vs time. For the polymerization with lower ligand concentration, the rate of polymerization was significantly slower than that of Re−Sty (entry 8, $k_{app} \sim 4.5 \times 10^{-6}$ s^{-1}). However, when 2 equiv of ligand was used, the reaction rate increased substantially (entry 9, $k_{app} \sim 2.7 \times 10^{-5}$ s^{-1}). We do not fully understand this phenomenon and suggest that higher ligand concentration may enhance the solvation

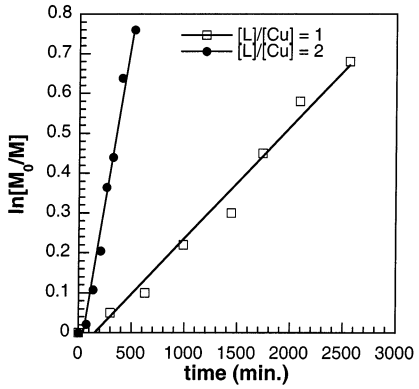

Figure 8. Plot of ln [M_0/M] vs time for the bulk polymerization of Sty at 95 °C initiated by complex **5** with different ligand concentrations. $[Sty]_0 = 8.7$ M (bulk); $[CuBr]_0 = 0.05$ M; $[\mathbf{5}]_0 = 0.025$ M.

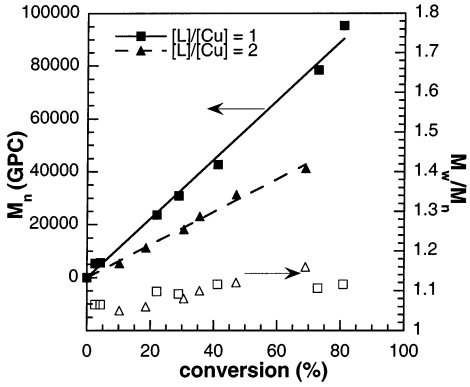

Figure 9. Plot of M_n and M_w/M_n vs conversion for the bulk polymerization of Sty at 95 °C initiated by complex **5** with different ligand concentrations. The filled data points are for M_n values and the open data points are for polydispersities. See Figure 8 for conditions.

of the growing polymer radical in the nonpolar styrene. The M_n vs conversion plots (Figure 9) show that the molecular weights increase linearly with conversion up to 80%, and the polydispersities remained low (1.12). The low polydispersity may also be attributed to the even lower solubility of ionic complex **5** in styrene. Such observations are consistent with those reported in the literature that insoluble initiator may become even less soluble as the polymerization proceeded than at the onset.[11]

Syntheses of Re—MMA and Ru—MMA. MMA was polymerized under the same condition as styrene. For the synthesis of Re−MMA, the reaction mixture became very viscous in 1.5 h. To lower the viscosity of the solution, xylene (1:1 w/w vs MMA) was used as the solvent for the reaction. The rate of the solution polymerization was slower than that of the bulk as expected. The kinetic plots (Figure 10) of both bulk and solution polymerizations show first-order reactions ($k_{app} = 1.7 \times 10^{-4}$ and 5.1×10^{-5} s^{-1}, respectively). For the synthesis of Ru−MMA, initiator **5** was more soluble in bulk MMA and hence had a significantly faster reaction rate ($k_{app} = 3.8 \times 10^{-4}$ s^{-1}) than that of Re−MMA.

Metal Complexes as Photosensitizers. The metal complex cores in the polymers can act as photosensitizers. By using ATRP, the molecular sizes of these polymers can be accurately controlled, and therefore, the density of these sensitizers can be adjusted. In addition, the complexes are encapsulated within a relatively nonpolar polymer matrix, and the photo-

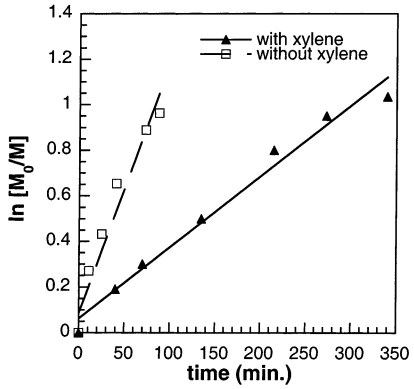

Figure 10. Plot of ln $[M_0/M]$ vs time for the polymerization of MMA at 40 °C initiated by complex **3** for bulk and solution polymerization. For bulk polymerization: $[MMA]_0 = 9.3$ M; $[CuBr]_0 = [PMDETA]_0 = 2[\mathbf{3}]_0 = 0.053$ M. For solution polymerization: $[MMA]_0 = 4.6$ M (xylene solution); $[CuBr]_0 = [PMDETA]_0 = 2[\mathbf{3}]_0 = 0.026$ M.

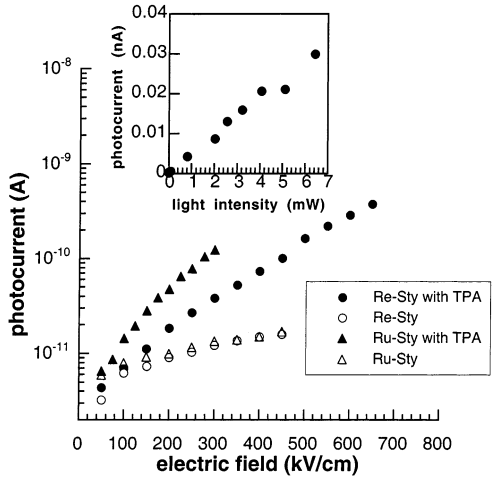

Figure 11. Photocurrent responses of Re−Sty and Ru−Sty at 488 nm with and without doping with TPA. Inset: A plot of photocurrent response as the function of light intensity under an applied electric field of 100 kV/cm.

sensitizing units are evenly distributed. This provides a good model for studying the effect of distribution of photosensitizers to the resulting photoconductivity. The photosensitizing properties of the polymers were studied by measuring the photocurrent response upon irradiation of light at 488 nm where the complexes strongly absorb. Although previous results showed that some of these complexes are potentially charge transport species, their concentrations are too low to provide an effective charge transport process.[16] Triphenylamine (30% w/w) was added in order to enhance the charge carrier mobilities. Figure 11 shows the photocurrent response of the doped and undoped Re−Sty and Ru−Sty. Upon addition of triphenylamine, the photocurrent responses are 1 order of magnitude higher than those of the undoped polymers. Their photoconductivities are on the order of 10^{-10} Ω^{-1} cm^{-1}, and the quantum yields are on the order of 10^{-6} (Table 4). In general, polymers with ruthenium complex cores show larger photocurrent responses. Nevertheless, the differences between rhenium and ruthenium containing polymers are not significant. These results are comparable to triphenylamine doped polycarbonate films irradiated with UV light.[29] A plot of photocurrent vs light intensity (Figure 11, inset diagram) is linear, showing clearly that the

Table 4. Photoconducting Properties of Polymers Doped with Triphenylamine (30 wt % and the Onsager Fitting Results

polymer	photoconductivity, σ^a (10^{-11} Ω^{-1}cm^{-1})	quantum yield, $\Phi \times 10^{-6}$ [a]	primary yield, $\Phi_0 \times 10^{-2}$	thermalization distance, r_0 (nm)
Re−Sty	10.1	1.2	3.0	1.3
Re−MMA	5.4	3.7	2.6	1.5
Ru−Sty	20	6.9	1.7	1.8
Ru−MMA	34	2.7	0.4[b]	2.3[b]

[a] Photoconductivity and quantum yield of the polymers were measured under an applied electric field of 450 kV/cm. [b] Experimental data points were not well fitted to Onsager's equation.

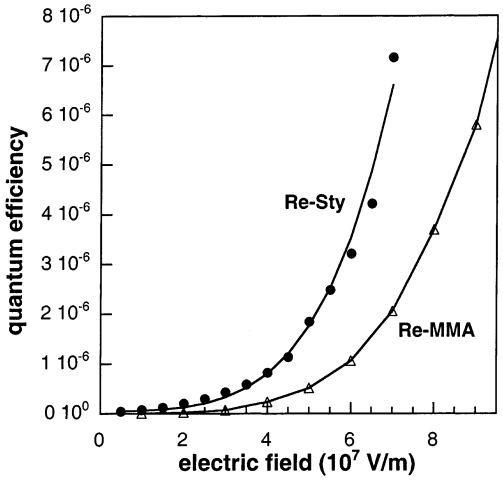

Figure 12. Plot of experimental quantum efficiency for Re−Sty and Re-MMA doped with TPA. The solid lines are the theoretical curves for $\Phi(r_0, E)$ as the function of applied electric field.

enhancement in photoconductivity is due to light irradiation.

The electric field dependent charge generation and separation process is described well by Onsager's theory of germinate recombination.[30] This theory assumes that some fraction of absorbed photons produce bound thermalized electron−hole pairs which either recombine or dissociate under the combined effects of the Coulombic attraction and the electric field. The photogeneration efficiency is given as the product of the quantum yield of thermalized pair formation and the pair dissociation probability:

$$\Phi(r_0, E) = \Phi_0\left[1 - \left(\frac{eEr_0}{kT}\right)^{-1}\sum_{g=0}^{\infty} I_g\left(\frac{e^2}{4\pi\epsilon_0\epsilon_r kTr_0}\right) I_g\left(\frac{eEr_0}{kT}\right)\right] \quad (1)$$

where I_g is a recursive formula given by

$$I_{g+1}(x) = I_g(x) - x^{g+1}\exp(-x)/(g+1)! \quad (2)$$

with $I_0(x) = 1 - \exp(-x)$, Φ_0 is the primary yield of thermalized bound pairs, r_0 is the initial thermalization separation between the bound charges, ϵ_0 is the permittivity of free space, ϵ_r is the relative permittivity, and E is the applied electric field strength. By fitting of the field-dependent experimental quantum yield Φ into eq 1, important parameters such as the primary yield Φ_0 and the thermalization distance r_0 can be obtained.

The experimental quantum yield of Re−Sty and Re−MMA with TPA were fitted into Onsager's equation.

Figure 12 shows the best fit of experimental results for these polymers. The primary yield and thermalization distance obtained from the fitting results are approximately 0.02 and 1.3−1.8 nm, respectively. Again, these data are very similar to polycarbonate films doped with isopropylcarbazole or triphenylamine.[29,31] This suggests that the excitons are localized near the site of photoexcitation, and the Φ_0 and r_0 values are largely dependent on the TPA dopant. The metal complexes mainly enhanced the photosensitivities of the polymers in the visible region and were not involved in the charge separation/transport processes.

Conclusions

Different PS and PMMA derivatives containing metal complex cores were successfully synthesized by ATRP using the CuBr/PMDETA as the catalyst system with rhenium and ruthenium complexes as the initiators. The molecular weight of the polymers can be estimated from their NMR spectra by comparing the integrals of the protons due to the initiators and the monomer units. The polymerization kinetics confirmed that the reactions were first order in monomer. The reaction rates depended on the amount of ligand, the initiators, and the nature of the initiators. The photocharge generation processes were studied in detail by measuring the photocurrent response of the undoped and doped polymers. When the polymers were doped with a hole transporting triphenylamine, an enhancement in photoconductivity in the visible region was observed, indicating that the metal complexes mainly serve as photosensitizers instead of charge carriers.

Acknowledgment. The work reported in this paper is substantially supported by The Research Grants Council of The Hong Kong Special Administrative Region, China (Project Nos. HKU 7096/00P and 7095/01P). Partial financial support from the Committee on Research and Conference Grants and The Hung Hing Ying Physical Sciences Research Fund (University of Hong Kong) are also acknowledged.

Supporting Information Available: X-ray crystallographic files in CIF format for initiators **3** and **5**. This material is available free of charge via the Internet at http://pubs.acs.org.

References and Notes

(1) (a) Hawker, C. J.; Bosman, A. W.; Harthpp, E. *Chem. Rev.* **2001**, *101*, 3661. (b) Yamago, S.; Iida, K.; Yoshida, J. *J. Am. Chem. Soc.* **2002**, *124*, 2874. (c) Yamago, S.; Iida, K.; Yoshida, J. *J. Am. Chem. Soc.* **2002**, *124*, 13666. (d) Chong, Y. K.; Krstina, J.; Le, T. P. T.; Moad, G.; Postma, A.; Rizzardo, E.; Thang, S. H. *Macromolecules* **2003**, *36*, 2256. (e) Chiefari, J. C.; Mayadunne, R. T. A.; Moad, C. L.; Moad, G.; Rizzardo, E.; Postma, A.; Skidmore, M. A.; Thang, S. H. *Macromolecules*, **2003**, *36*, 2273.

(2) (a) Patten, P. T.; Matyjaszewski, K. *Adv. Mater.* **1998**, *10*, 901. (b) Matyjaszewski, K. *Macromolecules* **1999**, *31*, 4710. (c) Matyjaszewski, K.; Xia, J. *Chem. Rev.* **2001**, *101*, 2921. (d) Kamigaito, M.; Ando, T.; Sawamoto, M. *Chem. Rev.* **2001**, *101*, 3689.

(3) Patten, P. T.; Matyjaszewski, K. *Acc. Chem. Res.* **1999**, *32*, 895.

(4) Matyjaszewski, K.; Patten, T. E.; Xia, J. *J. Am. Chem. Soc.* **1997**, *119*, 674.

(5) (a) Gaynor, S. G.; Qiu, J.; Matyjaszewski, K. *Macromolecules* **1998**, *31*, 5951. (b) Matyjaszewski, K.; Nakagawa, Y.; Jasieczek, C. B. *Macromolecules* **1998**, *31*, 1535. (c) Pascual, S.; Coutin, B.; Tardi, M.; Polton, A.; Vairon, J.-P. *Macromolecules* **1999**, *32*, 1432. (d) Rademacher, J. T.; Baum, M.; Pallack, M. E.; Brittain, W. J.; Simonsick, W. J., Jr. *Macromolecules* **2000**, *33*, 284. (e) Chambard, G.; Klumperman, B.; German, A. L. *Macromolecules* **2000**, *33*, 4417. (f) de la Fuente, J. L.; Fernández-García, M.; Fernández-Sanz, M.; Madruga, E. L. *J. Polym. Sci., Part A: Polym. Chem.* **2001**, *39*, 3443. (g) de la Fuente, J. L.; Fernández-Sanz, M.; Fernández-García, M.; Madruga, E. L. *Macromol. Chem. Phys.* **2001**, *202*, 2565.

(6) (a) Ng, P. K.; Gong, X.; Wong, W. T.; Chan, W. K. *Macromol. Rapid. Commun.* **1997**, *18*, 1009. (b) Yu, S. C.;. Gong, X.; Chan, W. K. *Macromolecules* **1998**, *31*, 5639. (c) Ng, P. K.; Gong, X.; Chan, W. K. *Adv. Mater.* **1998**, *10*, 1337. (d) Ng, W. Y.; Gong, X.; Chan, W. K. *Chem. Mater.* **1999**, *11*, 1165. (e) Wong, C. T.; Chan, W. K. *Adv. Mater.* **1999**, *11*, 455. (f) Chan, W. K.; Ng, P. K.; Gong, X.; Hou, S. *J. Mater. Chem.* **1999**, 2103. (g) Yu, S. C.; Hou, S.; Chan, W. K. *Macromolecules* **1999**, *32*, 5251. (h) Yu, S. C.; Hou, S.; Chan, W. K. *Macromolecules* **2000**, *33*, 3273.

(7) (a) Chan, W. K.; Gong, X.; Ng, W. Y. *Appl. Phys. Lett.* **1997**, *71*, 2919. (b) Chan, W. K.; Ng, P. K.; Gong, X.; Hou, S. *Appl. Phys. Lett.* **1999**, *75*, 3920.

(8) Ng, P. K.; Gong, X.; Chan, S. H.; Lam, L. S. M.; Chan, W. K. *Chem.—Eur. J.* **2001**, *7*, 4358.

(9) (a) Hou, S.; Chan, W. K. *Macromol. Rapid Commun.* **1999**, *20*, 440. (b) Hou, S.; Man, K. Y. K.; Chan, W. K. *Langmuir* **2003**, *19*, 2485.

(10) (a) Angot, S.; Murthy, S.; Taton, D.; Gnanou, Y. *Macromolecules* **1998**, *31*, 7218. (b) Neumann, A.; Keul, H.; Höcker, H. *Macromol. Chem. Phys.* **2000**, *201*, 980. (c) Destarac, M.; Matyjaszewski, K.; Boutevin, B. *Macromol. Chem. Phys.* **2000**, *201*, 265. (d) Börner, H. G.; Beers, K.; Matyjaszewski, K.; Sheiko, S. S.; Möller, M. *Macromolecules* **2001**, *34*, 4375. (e) Moschogianni, P.; Pispas, S.; Hadjichristidis, N. *J. Polym. Sci., Part A*: *Polym. Chem.* **2001**, *39*, 650.

(11) Collins, J. E.; Fraser, C. L. *Macromolecules* **1998**, *31*, 6715.

(12) Johnson, R. M.; Corbin, P. S.; Ng, C.; Fraser, C. L. *Macromolecules* **2000**, *33*, 7404.

(13) (a) Fraser, C. L.; Smith, A. P.; Wu, X. *J. Am. Chem. Soc.* **2000**, *122*, 9026. (b) Wu, X. F.; Collins, J. E.; McAlvin, J. E.; Cutts, R. W.; Fraser, C. L. *Macromolecules* **2001**, *34*, 2812.

(14) (a) Schubert, U. S.; Eschbaumer, C.; Hien, O.; Andres, P. R. *Tetrahedron Lett.* **2001**, *42*, 4705. (b) Schubert, U. S.; Heller, M. *Chem.—Eur. J.* **2000**, *7*, 5252.

(15) Lam, L. S. M.; Chan, S. H.; Chan, W. K. *Macromol. Rapid Commun.* **2000**, *21*, 1081.

(16) (a) Lam, L. S. M.; Chan, W. K. *Chem. Phys. Chem.* **2001**, *2*, 252. (b) Chan, S. H.; Wong, W. T.; Chan, W. K. *Chem. Mater.* **2001**, *13*, 4635. (c) Djurišić, A. B.; Guo, W. L.; Li, E. H.; Lam, L. S. M.; Chan, W. K.; Adachi, S.; Liu, Z. T.; Kwok, H. S. *Opt. Commun.* **2001**, *197*, 355. (d) Lam, L. S. M.; Chan, W. K.; Djurišić, A. B.; Li, E. H. *Chem. Phys. Lett.* **2002**, *362*, 130.

(17) (a) Stufkens, D. J.; Vlček, A., Jr. *Coord. Chem. Rev.* **1998**, *177*, 127. (b) Rossenaar, B. D.; Stufkens, D. J.; Vlček, A., Jr. *Inorg. Chem.* **1996**, *35*, 2902.

(18) Gould, S.; Strouse, G. F.; Meyer, T. J.; Sullivan, B. P. *Inorg. Chem.* **1991**, *30*, 2942.

(19) Ng, W. Y.; Chan, W. K. *Adv. Mater.* **1997**, *9*, 716.

(20) Sheldrick, G. M. In *Crystallographic Computing 3*; Sheldrick, G. M., Kruger, C., Goddard, R., Eds.; Oxford University Press: Oxford, England, 1985; pp 175−189.

(21) Beurskens, P. T.; Admiral, G.; Beurskens, G.; Bosman, W. P.; de Gelder, R.; Israel, R.; Smits, J. M. M. *The DIRDIF-94 program system, Technical Report of the Crystallography Laboratory*; University of Nijmegen: Nijmegen, The Netherlands, 1994.

(22) Staal, L. H.; Oskam, A.; Vrieze, K. *J. Organomet. Chem.* **1979**, *170*, 235.

(23) (a) Dominey, R. N.; Hauser, B.; Hubbard, J.; Dunham, J. *Inorg. Chem.* **1991**, *30*, 4754. (b) Abel, E. W.; Dimitrov, V. S.; Long, N. J.; Orrell, K. G.; Osborne, A. G.; Pain, H. M.; Sik, V.; Hursthouse, M. B.; Mazid, M. A. *J. Chem. Soc., Dalton Trans.* **1993**, 597.

(24) (a) Rossenaar, B. D.; Kleverlaan, C. J.; van de Ven, M. C. E.; Stufkens, D. J.; Oskam, A.; Fraanje, J.; Goubita, K. *J. Organomet. Chem.* **1995**, *493*, 153. (b) Kirchhoff, J. R.; Kirschbaum, K. *Polyhedron* **1998**, *17*, 4033. (c) Winslow, L. N.; Rillema, D. P.; Welch, J. H.; Singh, P. *Inorg. Chem.* **1989**, *28*, 1596.

(25) Xia, J. H.; Matyjaszewski, K. *Macromolecules* **1997**, *30*, 7697.

(26) Lam, L. S. M.; Chan, W. K. Manuscript submitted for publication.

(27) Davis, K. A.; Matyjaszewski, K. *Macromolecules* **2000**, *33*, 4039.
(28) Johnson, R. M.; Ng, C.; Samson, C. C. M.; Fraser, C. L. *Macromolecules* **2000**, *33*, 8618.
(29) Borsenberger, P.; Contois, G.; Hoestery, D. *J. Chem. Phys.* **1978**, *68*, 637.
(30) Onsager, L. *Phys. Rev.* **1938**, *54*, 554.
(31) (a) Borsenberger, P.; Contois, G.; Hoestery, D. *Chem. Phys. Lett.* **1978**, *56*, 574. (b) Borsenberger, P.; Contois, G.; Ateya, A. *J. Appl. Phys.* **1979**, *50*, 914.

MA030161Y